On the Utility of Isotopic Fine Structure Mass Spectrometry in Protein Identification

ARTICLE *in* ANALYTICAL CHEMISTRY · APRIL 2012

Impact Factor: 5.64 · DOI: 10.1021/ac2034584 · Source: PubMed

4 AUTHORS, INCLUDING:

Mikhail V Gorshkov
Russian Academy of Sciences
77 PUBLICATIONS **1,241** CITATIONS
SEE PROFILE

Yury O Tsybin
École Polytechnique Fédérale de Lausanne
101 PUBLICATIONS **1,806** CITATIONS
SEE PROFILE

analytical chemistry

Article

pubs.acs.org/ac

On the Utility of Isotopic Fine Structure Mass Spectrometry in Protein Identification

Saša M. Miladinović,[†] Anton N. Kozhinov,[†] Mikhail V. Gorshkov,[‡] and Yury O. Tsybin*[,†]

[†]Biomolecular Mass Spectrometry Laboratory, Ecole Polytechnique Federale de Lausanne, 1015 Lausanne, Switzerland

[‡]Institute for Energy Problems of Chemical Physics, Russian Academy of Sciences, 119334 Moscow, Russian Federation

Supporting Information

ABSTRACT: Modern mass spectrometry (MS)-based protein identification and characterization relies upon accurate mass measurements of the ^{13}C isotopic distributions of the enzymatically produced peptides. Interestingly, obtaining peptide elemental composition information from its isotopic fine structure mass spectrum to increase the confidence in peptide and protein identification has not yet been developed into a bottom-up proteomics-grade analytical approach. Here, we discuss the possible utility and limitations of the isotopic fine structure MS for peptide and protein identification. First, we *in silico* identify the peptides from the *E. coli* tryptic digest and show the increased confidence in peptide identification by consideration of the isotopic fine structures of these peptides as a function of mass and abundance accuracies. In the following, we demonstrate that the state-of-the-art high magnetic field Fourier transform ion cyclotron resonance (FT-ICR) MS allows a routine acquisition of the isotopic fine structure information of a number of isobaric peptide pairs, including a pair of peptides originating from *E. coli*. Finally, we address the practical limitation of the isotopic fine structure MS implementation in the time-constraint experiments by applying an advanced signal processing technique, filter diagonalization method, to the experimental transients to overcome the resolution barrier set by the typically applied Fourier transformation. We thus demonstrate that the isotopic fine structures of peptides may indeed improve the peptide and possibly protein identification, can be produced in a routine experiment by the state-of-the-art high resolution mass spectrometers, and can be potentially obtained on a chromatographic time-scale of a typical bottom-up proteomics experiment. The latter one requires at least an order of magnitude increase in sensitivity of ion detection, which presumably can be realized using high-field Orbitrap FTMS and/or future generation of ultrahigh magnetic field FT-ICR MS equipped with harmonized ICR cells.

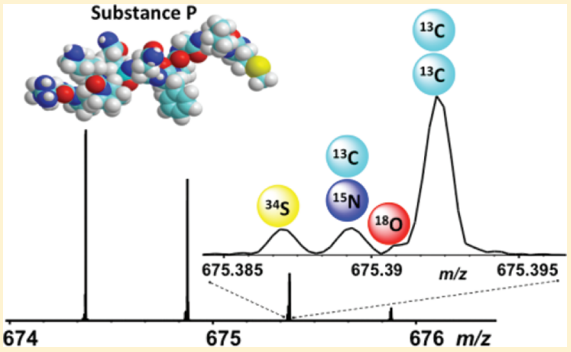

Mass spectrometry (MS) is one of the most efficient and versatile analytical tools for the comprehensive analysis of the samples of biological origin.[1,2] Within the palette of mass spectrometric methods utilized for such an analysis, Fourier transform ion cyclotron resonance mass spectrometry (FT-ICR MS) is a significant contributor to the biological research because of its high mass measurement accuracy, high resolving power, and unique tandem mass spectrometric (MS/MS) capabilities.[3−5] Since the introduction in 1974,[6] this type of mass spectrometry passed through a number of breaking developments[7] demonstrating unmatched resolving power until today. Examples include resolving of the $^{3}He^{+}/^{3}H^{+}$ isobaric ions at the peak resolution of 10 million and mass measurement accuracy of ~1 ppb[8] and 200 million peak resolution for $^{40}Ar^{+}$ ions and $^{132}Xe^{+}$ ions,[9] as well as 8 million for a protein.[10] In general, resolving powers in an excess of 1 million are routinely attainable for multiply charged peptides and proteins using high magnetic field FT-ICR MS technology. A comparable level of resolving power on other types of mass spectrometers became available recently with the development of high electrostatic field Orbitrap FTMS technology.[11,12] Specifically, Makarov and co-workers recently demonstrated resolution of up to 1 million for peptide ions on a chromatographic time scale of 3 s on the Orbitrap FTMS with the advanced signal processing, including phase correction, that corresponds to performance of modern high magnetic field FT-ICR mass spectrometers.[13]

The use of ^{13}C isotopic patterns produced by low resolution MS for improved molecular analysis has been suggested previously for light, <500 Da, molecules.[14] The achieved level of resolving power in FTMS thus provides the opportunity to have a deeper look at the isotopic pattern of detected ion elemental composition in search of a more reliable way of peptide identification. Indeed, Shi et al. and Miura et al. have shown that the correct number of elements, such as S, O, and N, typically present in the elemental compositions of organic molecules, including peptides, can be determined if the resolving power of a mass spectrometer is sufficient enough for obtaining their relative isotopic abundances.[10,15] These high

Received: December 24, 2011
Accepted: April 2, 2012
Published: April 2, 2012

   dx.doi.org/10.1021/ac2034584 | *Anal. Chem.* 2012, 84, 4042−4051

resolution mass spectra are referred to as the "isotopic fine structures" to distinguish them from the peptide ^{13}C isotopic patterns which are attainable for most of the peptides with the majority of mass analyzers used in proteomics. However, even highly accurate isotopic fine structures cannot be used to distinguish between the peptide isomers. Therefore, information on the relative abundances of the isotopic fine structures should be considered as a source of information complementary to other sources, e.g., accurate mass, fragmentation pattern in MS/MS, retention time in liquid chromatography (LC), etc.

The commercially available FTMS platforms, ICR and Orbitrap, have already demonstrated the feasibility to obtain the isotopic fine structures of natural peptides and small proteins.[10,13,15−20] Knowing the number of chemical elements in a peptide may significantly reduce the number of possible elemental compositions assigned to an ion with a given mass accuracy.[21−23] However, despite the advantages of having additional information about the elemental compositions of the peptides, the isotopic fine structure has not been routinely employed in the existing protein identification strategies. There are several factors that limit the routine implementation of isotopic fine structure mass spectrometry. First, the resolving power required is typically in an excess of 1 million for most of the peptides, such as tryptic peptides considered in bottom-up proteomics. The required level of resolving power can be obtained by FTMS instruments but necessarily includes ion trapping in a spatially restricted area of an ion trap. The latter results in a strong influence of Coulombic interactions between the trapped ions on both the relative positions of the peaks in a mass spectrum originating from the ^{15}N, ^{34}S, and ^{18}O elements and the relative abundances of these peaks in the recorded fine structures. Second, to achieve the desired resolving power in the mass spectra, the FT-based ion trap technologies require extremely long experimental times, mostly due to the necessity of acquiring the time-domain signals in the 10 to 30 s range.[18] The above-mentioned limitations dictate the need to develop methods of ion frequency harmonics or multiples detection,[24] robust absorption-mode implementations,[25−28] and novel data processing tools, presumably non-FT based ones, aimed to overcome the resolution limitations of the FT algorithm.

Peptide identification from the *E. coli* tryptic digest has been previously analyzed *in silico* based on accurate mass measurements and isoelectric point calculations.[29] Here, we extend this early work and consider, through the *in silico* analysis of tryptic peptides generated from *E. coli* protein database, the utility of isotopic fine structure content in peptide mass spectra for improving the reliability of protein identification based on the bottom-up proteomic strategy. This utility is further investigated with the experimental examples in which we show the feasibility to obtain the isotopic fine structures for a number of pairs of natural and synthetic peptides with close m/z ratios by FT-ICR MS. Importantly, to overcome the experimental time limitations coming from the impractically slow scan rate in these high resolution data acquisition sequences, we considered the possibility to process the time-domain transients with the filter diagonalization method (FDM) instead of the FT-based one.[30] The FDM method was recently introduced for FT-ICR mass spectrometry by O'Connor and co-workers for frequency tracing along the time-domain transient signals.[31,32] Furthermore, O'Connor successfully demonstrated the possibility of employing FDM for obtaining isotopic fine structures from significantly shorter, yet simulated, time-domain signals compared with a common FT-based approach.[31] The first application of FDM-based mass spectrometry to the experimental data, termed FDM MS, has recently been shown by our group to resolve ^{13}C isotopic structures of small molecules, peptides, and proteins using shorter transient time-domain signals compared to the FT-based signal processing.[33]

EXPERIMENTAL SECTION

Samples and Sample Preparation. Standard peptides, bradykinin ($C_{50}H_{73}N_{15}O_{11}$, monoisotopic mass 1059.5614 Da) and substance P ($C_{63}H_{98}N_{18}O_{13}S$, monoisotopic mass 1346.7281 Da), were purchased from Sigma-Aldrich (Buchs, Switzerland) and used without further purification. Peptide H-VGPPGFSPFVG-OH ($C_{52}H_{73}N_{11}O_{13}$, bradykinin isobar, monoisotopic mass 1059.5389 Da), isobaric pair H-RVMRGMR-OH ($C_{35}H_{68}N_{16}O_8S_2$, monoisotopic mass 904.4847 Da) and H-RSHRGHR-OH ($C_{35}H_{60}N_{20}O_9$, monoisotopic mass 904.4852 Da), and two isobaric peptides from *E. coli* tryptic digest, annotated in the manuscript as *E. coli* peptide 1 (H-ITNHHDHATGDIQTIGHHFR-OH, $C_{99}H_{147}N_{35}O_{30}$, monoisotopic mass 2306.1053 Da) and *E. coli* peptide 2 (H-KPIWENQSCDTSNLMVLNSK-OH, $C_{98}H_{159}N_{27}O_{33}S_2$, monoisotopic mass 2306.1035 Da), were synthesized in-house by solid-state Fmoc chemistry (Peptide and Protein Synthesis Facility, University of Lausanne, Switzerland). HPLC-MS grade water and acetonitrile were obtained from Fluka (Buchs, Switzerland). Formic acid was obtained from Merck (Zug, Switzerland). Peptides were dissolved in water and acetonitrile (50/50, v/v) with addition of 0.5% of formic acid to make 1−5 μM solutions.

Mass Spectrometry. Peptides were ionized using conventional microelectrospray ionization (ESI) ion source. Mass spectrometric measurements were performed using a hybrid 10 T linear ion trap Fourier transform ion cyclotron resonance mass spectrometer (LTQ FT-ICR MS, Thermo Scientific, Bremen, Germany), described elsewhere.[34] The experimental parameters and sequences were controlled by Xcalibur software (Thermo Scientific). Ions in question were first isolated in the LTQ with an isolation window of 5 m/z and then transferred to the capacitively coupled cylindrical ICR cell (Ultra cell, Thermo Scientific) followed by gated trapping at 3 V potentials applied to the trapping electrodes of the ICR cell. The trapping potentials were kept at 3 V during ion excitation event and then reduced to 0.4 V for ion detection.[34] The number of accumulated ions was controlled with the automatic gain control (AGC) function, which was set to 5×10^5 charges in the LTQ, unless stated otherwise. An ion relaxation period in the ICR cell of up to 1 s was followed by broadband frequency-sweep excitation to a post-excitation radius corresponding to approximately half of the cell's radius. Final time-domain (transient) signals were obtained by summation of 100 single transients of about 12 s long each. Unless stated otherwise, the MIDAS software package (National High Magnetic Field Laboratory, FL, USA) was employed to process the resulted transient signals in a conventional way with a single zero-filling, Hanning apodization and fast Fourier transform (FFT) to produce magnitude-mode frequency spectrum and convert it into the final mass spectrum using external calibration.[35]

The mass and abundance measurement accuracies were calculated based on the standard approaches.[34,36] Briefly, the mass or m/z accuracy (error, in ppm) and the abundance accuracy (error, in %) for a given ion peak were obtained according to the following expressions respectively

dx.doi.org/10.1021/ac2034584 | Anal. Chem. 2012, 84, 4042−4051

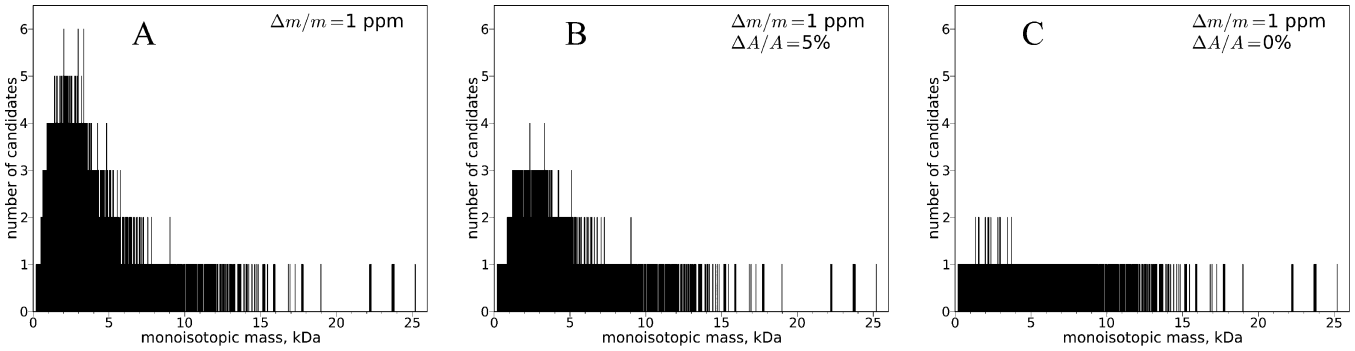

Figure 1. Number of possible candidates for the peptide elemental composition as a function of the peptide monoisotopic mass in identification of *E. coli* tryptic peptides based on the measurement of the monoisotopic masses with 1 ppm mass accuracy alone (A) and with the additional information of the relative abundance of the ^{15}N ion peaks compared to the ^{13}C ones with the 5% (B) and 0% (C) abundance accuracy.

$$\frac{\Delta(m/z)}{m/z} = \frac{(m/z)_{exp} - (m/z)_{th}}{(m/z)_{th}}, \quad \frac{\Delta A}{A} = \frac{A_{exp} - A_{th}}{A_{th}}$$

where $(m/z)_{exp}$ is the experimental mass-to-charge ratio of the considered peak, A_{exp} is the experimental relative abundance of the peak (compared to either ^{13}C peak for A+1 isotopic fine structure or $^{13}C_2$ peak for A+2 isotopic structure), and $(m/z)_{th}$ and A_{th} represent the corresponding theoretical values calculated using masses and natural abundances of isotopes (National Institute of Standards and Technology, 2010).[37] Errors, that could be referred to as total errors, of experimental m/z and abundance values include systematic and random errors. In the current work summation of 100 transient signals for each mass spectrum with isotopic fine structure was employed and resulted in random errors of relative abundances to be typically below the systematic ones in the control experiments with bradykinin and its isobaric peptide (see Results and Discussion section) so that the total errors are mainly systematic. See the Supporting Information for details on random error determination procedure. Note, for ^{13}C isotopic distributions the total error of relative abundance measurement was reported to be about 1% in case of summation of 100−200 transients for the employed FT-ICR mass spectrometer.[34]

Method Development. The in-house developed Python-based library, PyFTMS, was employed to perform *in silico* digestion procedure of the *E. coli* proteins (based on the UniProt repository); select peptides from the obtained digest for given mass and abundance measurement accuracies; calculate theoretical isotopic fine structures for selected peptides; and carry out peptide identification based on matching theoretical and experimental data. The isotopic distribution is hereafter described with the monoisotopic peak denoted as "A", the first isotopic cluster corresponding to a single ^{13}C isotope as "A+1", the second one corresponding to 2 atoms of ^{13}C present as "A+2", etc. Examining the experimental isotopic fine structures could potentially be used to estimate the numbers of atoms of a certain element in the peptide elemental composition. For example, the relative number of nitrogen atoms compared to the number of carbon ones corresponds to the abundance of the ^{15}N peak compared to the ^{13}C one in the A+1 isotopic fine structure cluster.[10]

Finally, PyFTMS was used to obtain mass spectra of A+1 isotopic fine structure of selected ions for different lengths of the experiential transient signal using signal processing based on Fourier transform and filter diagonalization method (FDM). The former was performed in a conventional way. The latter followed a typical FDM routine[30] and FDM MS methodology described elsewhere.[33] Briefly, with a chosen number of basis functions as a constraint of the algorithm, FDM calculations were performed for a selected frequency (mass-to-charge) window to find a number of parameters, including frequencies and amplitudes, of signal components from ions of interest. Note, the number of basis functions should exceed the number of peaks of interest in the considered window.[30] In the current work, the number of basis functions was selected based on the expected A+1 isotopic fine structure, albeit in general it can be chosen based on other parameters, e.g., stability of the calculations performed for a set of different numbers of basis functions if there is no information on the analyzed sample and experimental conditions. Based on the frequencies and amplitudes, a Lorentzian shape spectrum in the frequency scale is created with user-defined peak width and converted into a mass spectrum using the standard external calibration. Profiling a frequency spectrum is employed only for visual convenience, whereas the reported m/z ratios and abundances are obtained directly from the frequencies and amplitudes using the standard external calibration.[33]

RESULTS AND DISCUSSION

Analysis of Peptide Isotopic Fine Structure Utility in Proteomics. The *in silico* identification of *E. coli*-derived tryptic peptides was employed here to evaluate the utility of peptide isotopic fine structure information in the large-scale proteomic studies. Peptide identification based on the measurement of monoisotopic mass and relative abundance of ^{15}N peak compared to ^{13}C one from the A+1 isotopic fine structure was simulated. To characterize the performance of the technique depending on the experimentally provided mass and abundance measurement accuracies, the identification is considered for the sets of mass and abundance measurement accuracies, 0.1, 1, 5, 10 ppm and 0, 1, 2, 5, 10, 20, 50%, respectively. For a given mass accuracy, the potential of the technique was characterized by the abundance accuracy of 0% when the experimental errors in abundance measurements were absent. The distributions shown in Figure 1 and Figure S1 provide a number of possible candidates (vertical axis) for the peptide elemental composition as a function of the monoisotopic mass (horizontal axis) of the actual peptide subjected to the identification for considered mass and abundance measurement accuracies. In particular, Figure 1 shows a result of *in silico* peptide identification for mass accuracy of 1 ppm based on measurement of

dx.doi.org/10.1021/ac2034584 | *Anal. Chem.* 2012, 84, 4042−4051

Table 1. Analysis of *E. coli* Tryptic Digest Enzymatic Peptide Identification Based on Isotopic Fine Structure As a Function of Mass and Abundance Accuracy[a]

	Number of Elemental Compositions Distributed into Mass Bins with N Candidates											
	10 ppm mass accuracy						5 ppm mass accuracy					
abundance accuracy, %	$N = 1$	$N = 2$	$N = 3$	$3 < N \leq 6$	$6 < N \leq 14$	$14 < N \leq 22$	$N = 1$	$N = 2$	$N = 3$	$3 < N \leq 6$	$6 < N \leq 14$	$14 < N \leq 22$
NA	15647	13942	13349	38973	67689	3232	29972	26177	25314	56119	15250	0
50	16217	14704	13769	39667	65493	2982	30766	26894	25776	54999	14397	0
20	23732	21155	18894	45061	43463	527	44104	38878	26814	37923	5113	0
10	42530	34466	24336	40639	10860	1	63434	46776	24878	17238	506	0
5	78900	36462	19742	16868	860	0	101043	38194	11081	2511	3	0
2	116362	27608	7164	1698	0	0	135839	15916	1039	38	0	0
1	133135	17421	2066	210	0	0	148174	4589	68	1	0	0
0	142488	9902	441	1	0	0	152542	288	2	0	0	0
	1 ppm mass accuracy						0.1 ppm mass accuracy					
abundance accuracy, %	$N = 1$	$N = 2$	$N = 3$	$3 < N \leq 6$	$6 < N \leq 14$	$14 < N \leq 22$	$N = 1$	$N = 2$	$N = 3$	$3 < N \leq 6$	$6 < N \leq 14$	$14 < N \leq 22$
NA	103835	39508	8378	1111	0	0	151358	1468	6	0	0	0
50	105487	38418	7898	1029	0	0	151366	1460	6	0	0	0
20	121257	27366	3791	418	0	0	152321	511	0	0	0	0
10	137828	14458	526	20	0	0	152757	75	0	0	0	0
5	139991	12569	269	3	0	0	152806	26	0	0	0	0
2	143885	8855	92	0	0	0	152814	18	0	0	0	0
1	150708	2110	14	0	0	0	152818	14	0	0	0	0
0	152804	28	0	0	0	0	**152832**	0	0	0	0	0

[a]A complete mass range of 1-25 kDa, comprising all *in silico* produced enzymatic peptides (152832 elemental compositions), is considered.

monoisotopic mass only (Figure 1 A) and with relative abundances of ^{15}N to ^{13}C peaks measured with abundance accuracy, $\Delta A/A$, of 5% (Figure 1 B) and 0% as the upper limit case (Figure 1 C). Table 1 and Table S1 provide distributions of the total numbers of the elemental compositions over the mass bins in Figure 1 and Figure S1 with different numbers of candidates inside for the considered mass and abundance measurement accuracies. The total number of possible elemental compositions considered for a mass range of 0 to 25 kDa (all tryptic peptides are included) was 152832 (Table 1) and for a mass range of 1 to 7 kDa (truncated distribution of tryptic peptides) was 132289 (Table S1). Therefore, more than 86% of all elemental compositions of tryptic peptides from *E. coli* were within 1 to 7 kDa mass range.[29]

For both mass regions, the mass measurement accuracy of 1 ppm was not sufficient for the unambiguous *E. coli* peptide elemental composition identification based upon the peptide mass measurement alone.[29] Depending on the monoisotopic mass of the peptide, the number of possible candidates varies between 1 and 6. We expect these numbers to be significantly higher for the peptide databases of more complex organisms. The ambiguity of the identification varies as a function of both mass and abundance accuracies and reduces as the abundance accuracy improves for a given mass accuracy, as expected. The presented results allow estimation of the required abundance accuracy threshold for a desired false discovery rate. Finally, all peptide elemental compositions could be uniquely identified only for the mass accuracy of 0.1 ppm and abundance accuracy of 0%, among the presented cases for both mass ranges so that all elemental compositions go to the different bins. This analysis could be further generalized by taking into account relative abundances of other isotopic ions, such as sulfur and oxygen.

The analytical utility of peptide isotopic fine structure in proteomics could be compared to the utility of peptide isotopic structure that considers the abundance of the unresolved ^{13}C isotopic peaks. Fiehn and co-workers demonstrated that relative abundance of isotopic peaks of organic molecules of up to 500 Da acquired on a low-resolution MS can improve molecular identification by providing information on their elemental composition.[14] However, proteolytic peptides considered in the current work possess more complicated isotopic structure. Application of low-resolution MS to quantify the ratio of abundances of monoisotopic and ^{13}C-containing isotopic peaks will result in substantially higher error than for the small molecules. Furthermore, to quantitatively compare the utility of isotopic fine structure and ^{13}C isotopic structure in peptide identification, we complemented the results presented above by the *in silico* identification of *E. coli*-derived tryptic peptides based on the measurement of the relative abundance of ^{13}C peak from the A+1 isotopic cluster compared to the monoisotopic peak, see Figure S2 and Tables S2 and S3. The methodological and computational details are similar to the description of the data presented above for isotopic fine structure calculations. The results demonstrate the overall superiority of isotopic fine structure information to the ^{13}C isotope information in peptide elemental composition assignment. Therefore, high resolution MS that resolves peptide isotopic peaks to the level of isotopic fine structure shall (i) improve the performance of the ^{13}C isotope-based molecular structure analysis by reducing the abundance errors and (ii) provide complementary information to further reduce the number of possible peptide candidates.

Isotopic Fine Structures of Bradykinin and Its Isobaric Peptide. FT-ICR mass spectra of the two isobaric peptides, bradykinin and H-VGPPGFSPFVG-OH, were obtained with the resolving power of 1,500,000 at m/z 1061, Figure 2. Mass difference between the monoisotopic masses (denoted as "A" peaks) of these singly protonated (or neutral) peptides is only 22.47 mDa, Figure 2 A. The obtained resolving power was

dx.doi.org/10.1021/ac2034584 | *Anal. Chem.* 2012, 84, 4042–4051

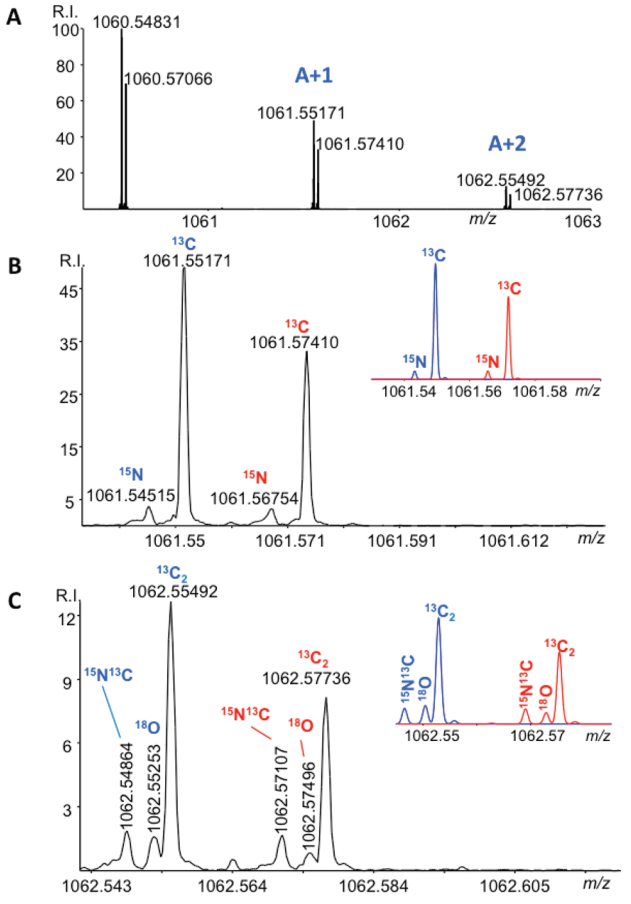

Figure 2. ESI FT-ICR MS of bradykinin and H-VGPPGFSPFVG-OH peptide pair showing (A) the ^{13}C isotopic envelope of the singly charged peptides and the expanded segments of this mass spectrum demonstrating (B) the isotopic fine structure of the A+1 isotopic envelope and (C) the isotopic fine structure of the A+2 isotopic envelope. Ion signals corresponding to bradykinin are shown in red (the heavier peptide) and to the H-VGPPGFSPFVG-OH peptide in blue (the lighter peptide). Abundance accuracies of the experimental values versus the theoretical ones are shown in Table 2, whereas the insets represent the theoretical isotopic fine structure distributions.

sufficient to resolve the isotopic fine structures corresponding to the natural abundances of ^{13}C, ^{15}N, and ^{18}O elements in the A+1 and A+2 isotopic envelopes of these peptides. The A+1 isotopic envelopes of singly protonated peptides reveal the presence of both ^{13}C and ^{15}N isotopic peaks, Figure 2 B, whereas the A+2 isotopic envelops are composed of ^{13}C, $^{15}N^{13}C$, and ^{18}O isotopes, Figure 2 C. The theoretical isotopic fine structures are shown in the insets in Figures 2 B and 2 C, respectively. Theoretically, 15 nitrogen atoms in bradykinin should give the ^{15}N isotopic peak relative abundance of 10.13% compared to the neighboring ^{13}C isotopic peak. At the same time, the synthetic peptide from this pair contains 11 nitrogen atoms providing the ^{15}N isotopic peak relative abundance of 7.15%, Figure 2 B inset. Accordingly, the ratio of $^{15}N^{13}C$ to $^{13}C_2$ ion abundances in these isotopic fine structure envelopes equals to 20.68% for bradykinin ion and 14.6% for the synthetic one, Figure 2 C inset. The ^{18}O signal is present in A+2 isotopic envelope and theoretical abundances versus the corresponding $^{13}C_2$ are 15.8% and 17.2% for bradykinin and synthetic peptide, respectively.

The accuracies of experimental relative abundances for the peaks in the A+1 and A+2 isotopic fine structure envelopes of bradykinin and its isobaric peptide are summarized in Table 2 (see the Experimental Section and the Supporting Information for more details). The effects that influence the ion signal abundances in FTMS have been described previously.[21,38−41] In most cases, the $\Delta A/A$ values are relatively small and are in the range of 0.2%−5%, Table 2. However, for the ^{18}O isotopic peaks the abundance errors are 26% and 34% for the synthetic peptide and bradykinin, respectively. The main contribution in such big errors is most probably due to spectral interference[42] since the ^{18}O isotopic peaks are resolved insufficiently, Figure 2 C. The random errors of relative abundances in a single FT-ICR MS measurement comprising of 100 summed single time-domain transient signals were estimated based on the spectral signal-to-noise ratio (SNR), see the Supporting Information for more details. As expected, for high abundance ^{15}N isotopic peaks the random errors were below 1%, Table 2. For low abundance ^{18}O isotopic peaks, the random errors were higher, up to 3%, since the signal-to-noise ratios of ^{18}O isotopic peaks are lower than the ones for the ^{15}N isotopic peaks.

The obtained accuracies of experimental abundances of ^{15}N isotopic peaks in the considered experiments (Table 2) show the instrumental performance in obtaining accurate abundances of the isotopic peaks in peptide identification based on A+1 isotopic fine structure, Table 1 and Table S1. From the obtained results it follows that FT-ICR MS is able to provide reasonable abundance accuracy of several percents once both systematic and random errors are paid attention to, so that the total error, which includes both systematic and random errors, is kept below a desired level. In particular, (i) at least baseline resolution is required to reduce systematic errors due to a detrimental effect of spectral interference and (ii) appropriate signal-to-noise ratios are needed to keep the random errors below the systematic errors once the latter ones are reduced down to a certain level.

Isotopic Fine Structures of E. coli Isobaric Tryptic Peptides. To evaluate the utility of the isotopic fine structure information in identification of peptides from complex mixtures containing isobaric peptides with masses within the 1 ppm window the *E. coli* tryptic digest was selected as a model system.[43] Figure 3 shows the high resolution FT-ICR MS-based analysis of the isotopic fine structures for a peptide pair for the triply charged peptides 1 and 2 from the *E. coli* tryptic digest (see the Experimental part for peptide sequences). The monoisotopic mass difference between these peptides in the neutral or singly charged state is 1.81 mDa. The m/z values of the monoisotopic peaks of the selected triply charged *E. coli* tryptic peptides, reported in Figure 3, differ only by 0.62 mTh, or 0.8 ppm in the relative m/z values, and thus represent a challenging case for the mass spectrometric identification. The high-resolution mass spectrometers are capable of resolving the corresponding ion signals, but mass measurement accuracy better than 0.8 ppm should be achieved to identify these two peptides based solely on the m/z values. The high magnetic field FT-ICR MS is able to resolve the isotopic fine structures for both peptides in this pair with the resolving power of 1.5 million, as shown in the expanded segments of the experimental mass spectrum in Figures 3 B and 3 C. It is known that the time-domain transient signal processing algorithms play a significant role in the resolving power and abundance accuracies achieved.[44] For example, Hanning apodization employed prior to Fourier transform to the experimental

dx.doi.org/10.1021/ac2034584 | *Anal. Chem.* 2012, 84, 4042−4051

Table 2. Mass Accuracies and Abundance Accuracies of Isotopic Fine Structure Distributions Obtained in the FT-ICR MS Measurements[a]

peptide	isotopic peak	$(m/z)_{exp}$	A_{exp}, %	$(m/z)_{th}$	A_{th}, %	mass accuracy, ppm	abundance accuracy, % (random error, %)
VGPPGFSPFVG	^{15}N	1061.54515	7.51	1061.54324	7.15	1.79	5.07 (0.68)
	^{13}C	1061.55171	N/A	1061.54956	N/A	2.03	N/A
	$^{15}N^{13}C$	1062.54864	14.8	1062.54660	14.6	1.92	1.35 (1.34)
	^{18}O	1062.55253	12.7	1062.55045	17.2	1.95	−26.1 (1.56)
	$^{13}C_2$	1062.55492	N/A	1062.55292	N/A	1.89	N/A
bradykinin	^{15}N	1061.56754	9.93	1061.56571	10.13	1.72	−1.96 (0.76)
	^{13}C	1061.57411	N/A	1061.57203	N/A	1.96	N/A
	$^{15}N^{13}C$	1062.57108	20.64	1062.56906	20.68	1.89	−0.18 (1.49)
	^{18}O	1062.57496	10.4	1062.57292	15.8	1.92	−33.9 (2.95)
	$^{13}C_2$	1062.57736	N/A	1062.57538	N/A	1.86	N/A
E. coli peptide 2	^{15}N	770.04223	11.6	770.04079	9.31	1.87	24.6
	^{13}C	770.04427	N/A	770.04290	N/A	1.78	N/A
	^{34}S	770.37511	12.8	770.37371	16.1	1.82	−20.5
	$^{15}N\ ^{13}C$	770.37668	14.4	770.37524	18.8	1.87	−23.4
	$^{13}C_2$	770.37872	N/A	770.37735	N/A	1.78	N/A
E. coli peptide 1	^{15}N	770.04301	9.8	770.04139	11.9	2.1	−17.9
	$^{13}C2$	770.0449	N/A	770.04350	N/A	1.82	N/A
	$^{15}N\ ^{13}C$	770.37762	20.7	770.37584	24.1	2.31	−14.2
	$^{13}C_2$	770.37935	N/A	770.37795	N/A	1.82	N/A
RVMRGMR	^{15}N	453.74859	20.8	453.74817	15.4	0.93	34.7
	^{13}C	453.75191	N/A	453.75133	N/A	1.29	N/A
	^{34}S	454.24819	153.3	454.24755	128.6	1.42	19.2
	$^{15}N\ ^{13}C$	454.25027	49.3	454.24984	31.8	0.94	55.1
	^{18}O	454.2524	26.7	454.25177	23.6	1.38	13
	$^{13}C_2$	454.2536	N/A	454.25300	N/A	1.31	N/A
RSHRGHR	^{15}N	453.74885	20.9	453.7484	19.3	0.99	8.28
	^{13}C	453.75229	N/A	453.75156	N/A	1.61	N/A
	$^{15}N\ ^{13}C$	454.25054	55	454.25008	39.7	1.02	38.4
	^{18}O	454.25272	20	454.25200	26.6	1.57	−24.7
	$^{13}C_2$	454.25388	N/A	454.25324	N/A	1.41	N/A

[a]The random abundance errors are provided, in the brackets, only for the experiments with bradykinin and H-VGPPGFSPFVG-OH peptide mixture (see the Experimental Section and the Supporting Information for more details). N/A indicates ^{13}C and $^{13}C_2$ peaks used as a reference in calculations of relative abundances.

transient did not completely resolve the ^{18}O isotopic peak from the $^{13}C_2$ one. The application of another type of the apodization function, Hamming apodization, provided better resolution of the A+2 isotopic pattern for the *E. coli* peptide 2, so that even the ^{18}O isotopic peak was resolved, see Figure S3 in the Supporting Information for more details. However, e.g., for the $^{15}N^{13}C$ isotopic peak of *E. coli* peptide 2 shown in Figure 3 and Figure S3, the abundance accuracy, $\Delta A/A$, of 37% was achieved when Hamming apodization was applied and −23.4% in the case of Hanning apodization. Therefore, Hanning apodization was used throughout the paper.[45] The abundance accuracies obtained in this way are reported in Table 2. The achieved abundance accuracies are limited by systematic errors and demonstrate a need for better resolution of the corresponding isotopic ions of the isobaric peptides.

Isotopic Fine Structures of Synthetic Isobaric Peptide Pair. Figure 4 shows the routine application of high magnetic field FT-ICR MS to a rationally designed pair of peptides, H-RVMRGMR-OH and H-RSHRGHR-OH. The monoisotopic mass difference between these peptides in the neutral or singly charged states is only 0.46 mDa. Figure 4 shows that the employed FT-ICR MS was not able to resolve the ^{13}C isotopic patterns of these peptides, as the monoisotopic peaks of the doubly charged ions differ in m/z only by 0.25 mTh (0.5 ppm). Previously, these peptides were baseline resolved with a record resolving power of ~3.3 million in a dedicated experiment by Marshall and co-workers and represent a case of the smallest, less than a mass of an electron (0.55 mDa), peptide mass difference resolved up to date.[46] Here, we routinely achieved the resolving power of ~2 million for this peptide pair when the peptides were doubly protonated. The resolving power achieved was sufficient to resolve the isotopic fine structures of both peptides, Figures 4 B and 4 C. Due to the presence of sulfur in one of the peptides in this pair, the ^{34}S peak in the isotopic fine structure can be an obvious marker of this peptide in the mixture. The abundance accuracies, experimental versus theoretical values of ^{13}C peak to ^{15}N peak ratio, for this peptide pair are reported in Table 2. The obtained isotopic fine structure information can potentially be used for peptide identification; however, the achieved abundance accuracies are significantly limited by a systematic error of spectral interference due to insufficient resolution of the same types of isotopic peaks of the isobaric peptides.

Toward Fast Acquisition of High Resolution Isotopic Fine Structures of Peptides. The 10 T FT-ICR MS transient signal length of at least 12 s and more is required to provide the

dx.doi.org/10.1021/ac2034584 | Anal. Chem. 2012, 84, 4042−4051

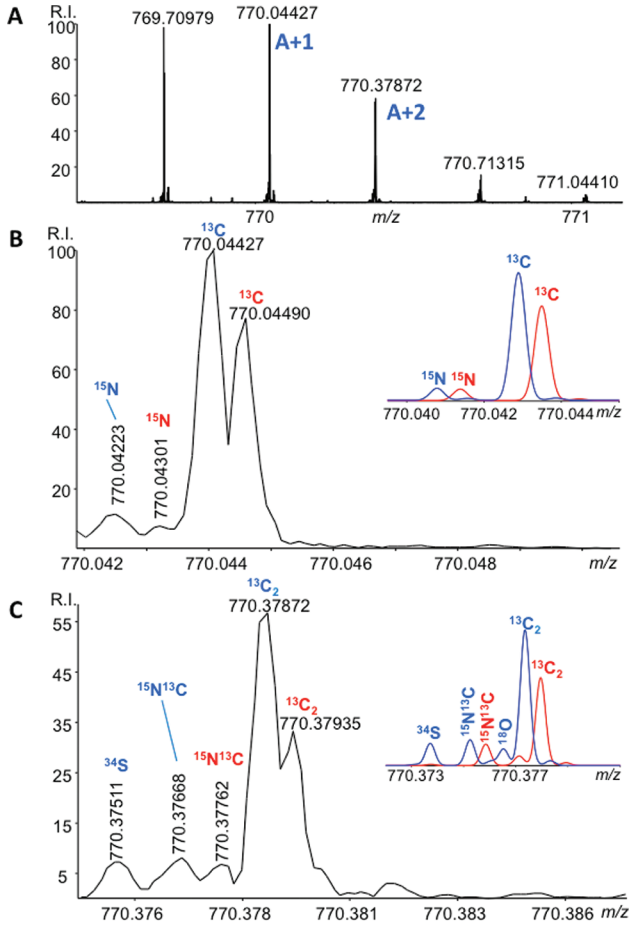

Figure 3. ESI FT-ICR MS of *E. coli* peptide pair showing (A) the ^{13}C isotopic envelope of the triply charged peptides and the expanded segments of this mass spectrum demonstrating (B) the isotopic fine structure of the A+1 isotopic envelope and (C) the isotopic fine structure of the A+2 isotopic envelope. Ion signals corresponding to the *E. coli* peptide 1 are shown in red (the heavier peptide) and to the *E. coli* peptide 2 in blue (the lighter peptide). Abundance accuracies of the experimental values versus the theoretical ones are shown in Table 2, whereas the insets represent the theoretical isotopic fine structure distributions.

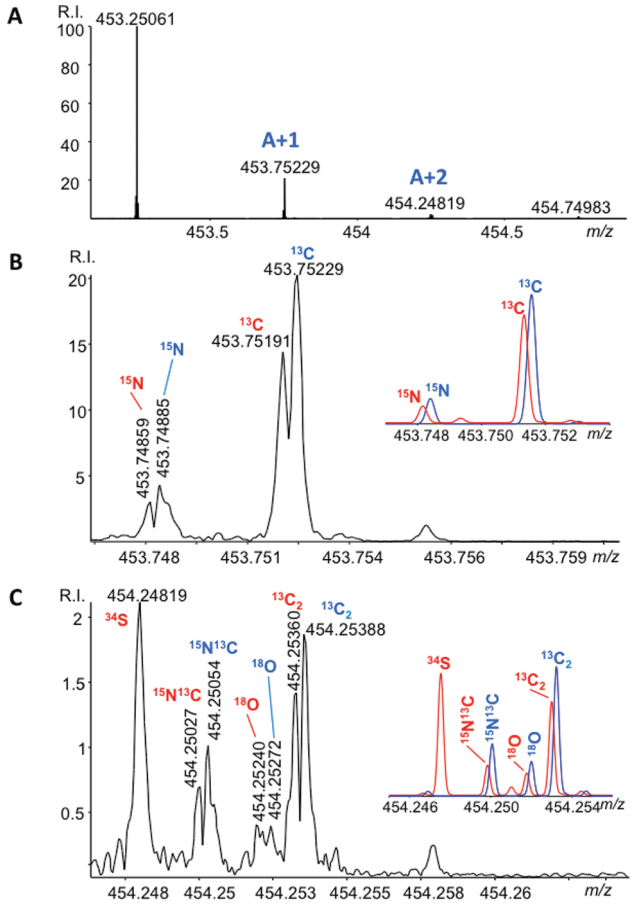

Figure 4. ESI FT-ICR MS of H-RVMRGMR-OH and H-RSHRGHR-OH peptide mixture showing (A) the ^{13}C isotopic envelope of the doubly charged peptides and the expanded segments of this mass spectrum demonstrating (B) the isotopic fine structure of the A+1 isotopic envelope and (C) the isotopic fine structure of the A+2 isotopic envelope. Ion signals corresponding to peptide H-RVMRGMR-OH are shown in red (the lighter peptide) and to H-RSHRGHR-OH peptide in blue (the heavier peptide). Abundance accuracies of the experimental values versus the theoretical ones are shown in Table 2, whereas the insets represent the theoretical isotopic fine structure distributions.

high resolution isotopic fine structure information for the isobaric peptide pairs, Figures 2-4. In case of isotopic fine structure measurements for a less complex ion mixture, such as single peptide ion, under the same experimental conditions, shorter acquisition time can be enough, nonetheless the one of several seconds and more is required, Figure S4 (Supporting Information). Even if a single transient provides a sufficient signal-to-noise ratio, such long acquisition times are impractical for the modern macromolecular analysis with the time constrains dictated by the LC-based rapid separation of peptide mixtures in the bottom-up proteomics. Therefore, the peptide isotopic fine structures must be obtained from not longer than ~1−2 s transients, which would be comparable with the typically obtained transient signals in the bottom-up proteomics and metabolomics by both ICR and Orbitrap FTMS. As introduced above, the filter diagonalization method, FDM, was selected as a method of advanced signal processing to accomplish this task. Figure 5 shows a comparison between FDM-based MS (FDM MS) and FFT (FTMS) processing of a time-domain transient signal of isolated singly charged ions of bradykinin and its isobaric peptide, Figure 2, acquired on a 10 T FT-ICR MS for different lengths of the signal. As expected, mass spectra from both FDM and FFT processing of 12.13 s transient signals revealed the isotopic fine structures of the A+1 isotope of bradykinin and its isobaric peptide, Figure 5 top. The FFT of a shorter, 1.66 s, initial portion of the recorded transient produced the mass spectrum without isotopic fine structure resolution. On the other hand, FDM of the same short transient signal revealed the isotopic fine structures, Figure 5 bottom. Even a less than 1 s transient signal can be sufficient for FDM-based signal processing to obtain the required information, see the results for a peptide substance P, Figure S4. Therefore, with FDM as a signal processing tool, the required length of a transient signal to obtain the isotopic fine structures of peptides in FT-ICR MS could be significantly reduced. Note, a signal perturbation is a characteristic of the time-domain transients followed by ion excitation event in FT-ICR MS.[32,47] The FDM processing of a part of the transient that contains these perturbations demonstrates a reduced method performance. Therefore, in Figure 5 and Figure S4 a time delay of, respectively, 0.16 and 1.0 s between ion

dx.doi.org/10.1021/ac2034584 | *Anal. Chem.* 2012, 84, 4042−4051

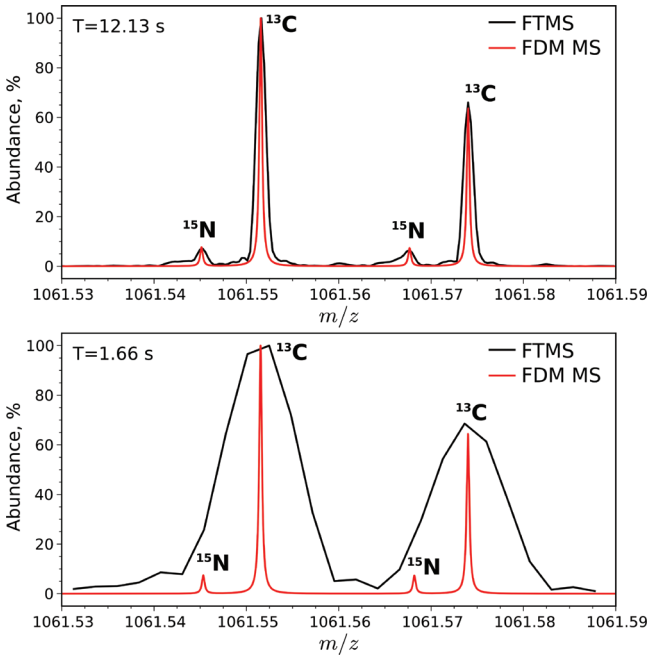

Figure 5. Comparison of super-resolution and Fourier transform signal processing to obtain the A+1 isotopic fine structure of singly protonated bradykinin and its isobaric peptide H-VGPPGFSPFVG-OH from the transient signal of 12.13 s length (top panel) and from its truncated version (1.66 s, bottom panel) using the conventional fast Fourier transform, FFT (shown in black and denoted as FTMS) and filter diagonalization method, FDM (shown in red and denoted as FDM MS). See Table 3 for more details. Bradykinin is a heavier peptide in this isobaric peptide pair.

excitation and detection was employed to exclude a part of the transient with the perturbations. The transient signal perturbation is significantly shorter in Orbitrap FTMS, due to the absence of the RF-excitation events. The bar-plot representation of the FDM MS data from Figure 5 is shown in Figure S5.

The mass accuracies and abundance accuracies for the data reported in Figure 5 are summarized in Table 3. The mass accuracies in both FTMS and FDM MS approaches suggest the systematic m/z error of the mass calibration to be the main contributor to the mass accuracy values, as in all previous experiments, Table 2. The abundance accuracies in the FTMS approach are consistent with the ones from the control experiments with bradykinin and its isobaric peptide. Note, the abundance measurement in the FDM MS approach is more accurate for shorter transients, Figure 5 bottom and top panels. The obtained abundance accuracies demonstrate the possible numerical effects of the FDM due to the insufficient quality of the transient signals. In general, the quality of transient signals is limited by (i) the space charge effects in the ICR cell,[32,48,49] (ii) imprecision and inharmonicity of the cylindrical ICR cell,[32,50] and (iii) insufficient signal-to-noise ratio, though it has been reported that FDM is relatively stable in case of noisy signals.[51] Therefore, the obtained results show the potential of FDM, once the transient signals of the appropriate quality are available, in obtaining isotopic fine structures in ICR MS, and, presumably, high-field Orbitrap FTMS,[12] on the LC-time scale. The computational resources required for FDM MS are substantially more significant than for the FTMS.[33] The FDM MS calculations performed in the current work required up to 30 min per single isotopic fine structure cluster calculations on a quad-core desktop computer. Therefore, application of FDM MS to large-scale LC/MS data sets requires a substantial increase in computational power. Luckily, the current FDM MS implementation allows method parallelization on multicore workstations.

CONCLUSIONS

The isotopic fine structures of the macromolecules, e.g., peptides and heavy metabolites, are the important source of structural information that is not currently being used in the routine MS workflows. Here, we have demonstrated that peptide identification in the bottom-up proteomics might be improved by considering the elemental composition information provided by the isotopic fine structure. Employing the high magnetic field FT-ICR MS for 3 pairs of isobaric peptides that differ in mass, within each pair, by 22.47 mDa, 1.81 mDa, and 0.46 mDa we have further shown that the current state-of-the-art high resolution MS is sufficient to achieve the required performance level and obtain this information in a relatively routine experiment. However, the time constraints of the modern MS experiments drastically limit the application of even the high magnetic field FT-ICR MS due to the long data acquisition time: more than 12 s were needed here to achieve the required resolution for the peptide pairs considered. The upcoming hardware developments, including even higher

Table 3. Mass Accuracies and Abundance Accuracies of Isotopic Fine Structure Distributions Obtained in the ICR MS Measurements of Bradykinin and H-VGPPGFSPFVG-OH Peptide Mixture Using FFT (Denoted as FTMS) and FDM (Denoted as FDM MS) Signal Processing[a]

			mass accuracy, ppm		abundance accuracy, %	
acquisition time, s	peptide	isotopic peak	FTMS	FDM MS	FTMS	FDM MS
12.13	H-VGPPGFSPFVG-OH	^{15}N	1.91	1.78	−0.1	6.18
		^{13}C	1.94	1.87	N/A	N/A
	bradykinin	^{15}N	1.83	1.84	−2.69	13.16
		^{13}C	1.86	1.87	N/A	N/A
1.66	H-VGPPGFSPFVG-OH	^{15}N	N/R	1.97	N/R	2.97
		^{13}C	N/R	1.86	N/A	N/A
	bradykinin	^{15}N	N/R	2.33	N/R	10.9
		^{13}C	N/R	1.85	N/A	N/A

[a]Notations are as follows: N/A − not applicable; N/R − not resolved. N/A indicates ^{13}C peaks used as a reference in calculations of relative abundances.

dx.doi.org/10.1021/ac2034584 | Anal. Chem. 2012, 84, 4042−4051

magnetic field FT-ICR MS equipped with harmonized ICR cells, as well as the recent implementation of high-field Orbitrap FTMS, present a strong potential for practical LC/MS by decreasing the experimental time and improving the sensitivity of ion detection at higher resolution. Complementarily, the recent advanced signal processing development accompanied by the substantial increase in the computation power accessible by a typical research laboratory together with the continuous progress in the MS hardware development show a significant promise for applications in large-scale LC/MS-based experiments. Importantly, we demonstrated here that the application of a filter diagonalization method, FDM, to the processing of the experimental FT-ICR MS transients of peptides allows resolving the peptide's isotopic fine structure from a less than 1−2 s transient signals. Thus, the isotopic fine structures of peptides could be potentially revealed by FDM in the common LC/MS analysis of complex peptide mixtures, where it is crucial to have a rapid MS analysis step, and used further to improve protein identification in bottom-up proteomics. We expect to achieve a similar or better level of performance of FDM signal processing for isotopic fine structure analysis on the Orbitrap FTMS transient signals.

■ ASSOCIATED CONTENT

Supporting Information

Additional information as noted in text. This material is available free of charge via the Internet at http://pubs.acs.org.

■ AUTHOR INFORMATION

Corresponding Author

*Phone: +41216939751. E-mail: yury.tsybin@epfl.ch. Corresponding author address: EPFL ISIC LSMB, BCH 4307, 1015 Lausanne, Switzerland.

Notes

The authors declare no competing financial interest.

■ ACKNOWLEDGMENTS

This work was supported by the Swiss National Science Foundation (project 200021-125147/1), Joint Research Project of Scientific & Technological Cooperation Program Switzerland-Russia (grant agreement 128357 between EPFL and INEPCP RAS), Russian Basic Science Foundation (project 11-04-00515 to M.V.G.), and European Research Council (ERC Starting Grant 280271 to YOT).

■ REFERENCES

(1) Domon, B.; Aebersold, R. *Science* **2006**, *312*, 212−217.
(2) Aebersold, R.; Mann, M. *Nature* **2003**, *422*, 198−207.
(3) Liu, T.; Belov, M. E.; Jaitly, N.; Qian, W.-J.; Smith, R. D. *Chem. Rev.* **2007**, *107*, 3621−3653.
(4) Tsybin, Y. O.; Quinn, J. P.; Tsybin, O. Y.; Hendrickson, C. L.; Marshall, A. G. *J. Am. Soc. Mass Spectrom.* **2008**, *19*, 762−771.
(5) Cooper, H. J.; Hakansson, K.; Marshall, A. G. *Mass Spectrom. Rev.* **2005**, *24*, 201−222.
(6) Comisarow, M. B.; Marshall, A. G. *Chem. Phys. Lett.* **1974**, *25*, 282−283.
(7) Marshall, A. G. *Int. J. Mass Spectrom.* **2000**, *200*, 331−356.
(8) Nikolaev, E. N.; Neronov, Y. I.; Gorshkov, M. V.; Talroze, V. L. *JETP Lett.* **1984**, *39*, 534−536.
(9) Knobler, M.; Wanczek, K. P. In *Proceedings of the 45th ASMS conference on mass spectrometry and allied topics*. Palm Springs, CA, June 1−5, 1997.
(10) Shi, S. D.-H.; Hendrickson, C. L.; Marshall, A. G. *Proc. Natl. Acad. Sci. U.S.A.* **1998**, *95*, 11532−11537.
(11) Makarov, A. *Anal. Chem.* **2000**, *72*, 1156−1162.
(12) Makarov, A.; Denisov, E.; Lange, O. *J. Am. Soc. Mass Spectrom.* **2009**, *20*, 1391−1396.
(13) Denisov, E.; Damoc, E.; Makarov, A.; Lange, O. In *Proceedings of the 59th ASMS conference on mass spectrometry and allied topics*. Denver, CO, June 5−9, 2011.
(14) Kind, T.; Fiehn, O. *BMC Bioinf.* **2006**, *7*, 234.
(15) Miura, D.; Tsuji, Y.; Takahashi, K.; Wariishi, H.; Saito, K. *Anal. Chem.* **2010**, *82*, 5887−5891.
(16) Gorshkov, M. V.; Pasa Tolic, L.; Udseth, H. R.; Anderson, G. A.; Bruce, J. E.; Prior, D. C.; Hofstadler, S. A.; Smith, R. D. In *Proceedings of the 46th ASMS conference on mass spectrometry and allied topics*. Orlando, FL, May 31-June 4, 1998.
(17) Miladinovic, S. M.; Kozhinov, A. N.; Gorshkov, M. V.; Tsybin, Y. O. In *Proceeding of the 59th ASMS conference on mass spectrometry and allied topics*. Denver, CO, June 5−9, 2011.
(18) Nikolaev, E.; Boldin, I.; Jertz, R.; Baykut, M. G. In *Proceedings of the 59th ASMS conference on mass spectrometry and allied topics*. Denver, CO, June 5−9, 2011.
(19) Tsybin, Y. O.; Fornelli, L.; Kozhinov, A. N.; Vorobyev, A.; Miladinovic, S. M. *Chimia* **2011**, *65*, 641−645.
(20) Blake, S. L.; Walker, S. H.; Muddiman, D. C.; Hinks, D.; Beck, K. R. *J. Am. Soc. Mass Spectrom.* **2011**, *22*, 2269−2275.
(21) Stoll, N.; Schmidt, E.; Thurow, K. *J. Am. Soc. Mass Spectrom.* **2006**, *17*, 1692−1699.
(22) Kim, S.; Rodgers, R. P.; Marshall, A. G. *J. Am. Soc. Mass Spectrom.* **2006**, *251*, 260−265.
(23) Zubarev, R. A.; Hakansson, P.; Sundqvist, B. *Anal. Chem.* **1996**, *68*, 4060−4063.
(24) Vorobyev, A.; Gorshkov, M. V.; Tsybin, Y. O. *Int. J. Mass Spectrom.* **2011**, *306*, 227−231.
(25) Beu, S. C.; Blakney, G. T.; Quinn, J. P.; Hendrickson, C. L.; Marshall, A. G. *Anal. Chem.* **2004**, *76*, 5756−5761.
(26) Xian, F.; Hendrickson, C. L.; Blakney, G. T.; Beu, S. C.; Marshall, A. G. *Anal. Chem.* **2010**, *82*, 8807−8812.
(27) Qi, Y. L.; Barrow, M. P.; Van Orden, S. L.; Thompson, C. J.; Li, H.; Perez-Hurtado, P.; O'Connor, P. B. *Anal. Chem.* **2011**, *83*, 8477−8483.
(28) Qi, Y.; Thompson, C. J.; Van Orden, S. L.; O'Connor, P. B. *J. Am. Soc. Mass Spectrom.* **2011**, *22*, 138−147.
(29) Cargile, B. J.; Stephenson, J. L., Jr. *Anal. Chem.* **2004**, *76*, 267−275.
(30) Mandelshtam, V. A. *Prog. Nucl. Magn. Reson. Spectrosc.* **2001**, *38*, 159−196.
(31) Aizikov, K.; O'Connor, P. B. *J. Am. Soc. Mass Spectrom.* **2006**, *17*, 836−843.
(32) Aizikov, K.; Mathur, R.; O'Connor, P. B. *J. Am. Soc. Mass Spectrom.* **2009**, *20*, 247−256.
(33) Kozhinov, A. N.; Tsybin, Y. O. *Anal. Chem.* **2012**, *84*, 2850−2856.
(34) Ben Hamidane, H.; Vorobyev, A.; Tsybin, Y. O. *Eur. J. Mass Spectrom.* **2011**, *17*, 321−331.
(35) Blakney, G. T.; Robinson, D. E.; Hgan, V. L.; Kelleher, N. L.; Hendrickson, C. L.; Marshall, A. G. In *Proceedings of the 53rd ASMS conference on mass spectrometry and allied topics*. San Antonio, TX, June 4−9, 2005.
(36) Blake, S.; Walker, S.; Muddiman, D.; Hinks, D.; Beck, K. *J. Am. Soc. Mass Spectrom.* **2011**, *22*, 2269−2275.
(37) http://www.nist.gov/pml/data/comp.cfm (accessed December 3, 2011).
(38) Gordon, E. F.; Muddiman, D. C. *J. Mass Spectrom.* **2001**, *36*, 195−203.
(39) Bresson, J. A.; Anderson, G. A.; Bruce, J. E.; Smith, R. D. *J. Am. Soc. Mass Spectrom.* **1998**, *9*, 799−804.
(40) Hofstadler, S. A.; Bruce, J. E.; Rockwood, A. L.; Anderson, G. A.; Winger, B. E.; Smith, R. D. *Int. J. Mass Spectrom. Ion Processes* **1994**, *132*, 109−127.
(41) Easterling, M. L.; Amster, I. J.; van Rooij, G. J.; Heeren, R. M. A. *J. Am. Soc. Mass Spectrom.* **1999**, *10*, 1074−1082.

(42) Kozhinov, A. N.; Miladinovic, S. M.; Tsybin, Y. O. In *Proceedings of the 59th ASMS conference on mass spectrometry and allied topics*. Denver, CO, June 5−9, 2011.
(43) Silva, J. C.; Denny, R.; Dorschel, C.; Gorenstein, M. V.; Li, G.-Z.; Richardson, K.; Wall, D.; Geromanos, S. J. *Mol. Cell. Proteomics* **2006**, *5*, 589−607.
(44) Marshall, A. G.; Verdun, F. R. *Fourier transforms in NMR, optical, and mass spectrometry: a user's handbook*. Elsevier: Amsterdam, 1990.
(45) Serreqi, A.; Comisarow, M. B. *Appl. Spectrosc.* **1987**, *41*, 288−295.
(46) He, F.; Hendrickson, C. L.; Marshall, A. G. *Anal. Chem.* **2001**, *73*, 647−650.
(47) Leach, F. E., III; Kharchenko, A.; Heeren, R. M. A.; Nikolaev, E.; Amster, I. J. *J. Am. Soc. Mass Spectrom.* **2010**, *21*, 203−208.
(48) Boldin, I. A.; Nikolaev, E. N. *Rapid Commun. Mass Spectrom.* **2009**, *23*, 3213−3219.
(49) Huang, J.; Tiedemann, P. W.; Land, D. P.; McIver, R. T.; Hemminger, J. C. *Int. J. Mass Spectrom. Ion Processes* **1994**, *134*, 11−21.
(50) Vladimirov, G.; Kostyukevich, Y.; Marshall, A. G.; Hendrickson, C. L.; Blackney, G. T.; Nikolaev, E. In *Proceedings of the 58th ASMS conference on mass spectrometry and allied topics*. Salt Lake City, UT, 2010.
(51) Benko, U.; Juricic, D. *Signal Process* **2008**, *88*, 1733−1746.